The L_{23}-$M_{4,5}M_{4,5}$ principal and satellite Auger spectra of Cu, Zn, and Ga

E. J. McGuire
Sandia Laboratories, Albuquerque, New Mexico 87115
(Received 8 June 1977)

The L_{23}-$M_{4,5}M_{4,5}$ principal and satellite Auger spectra are synthesized for atomic Cu and compared to the measurements in solid Cu. It is found that the L_2-$L_3M_{4,5}$ Coster-Kronig rate is significantly different in intermediate coupling from its value in j-j coupling. With intermediate coupling and matrix elements obtained with a Cu-ion potential (with an L-shell hole), the synthesized satellite spectra do not agree with the Cu measurements, but do agree with the measurements on Zn, when the energy scale is suitably contracted. With L_2-$L_3M_{4,5}$ matrix elements obtained with a neutral-atom Cu potential, the synthesized Cu spectra are in quantitative agreement with the measurements. However, in this case the calculated Cu L_2 linewidth is significantly larger than the measured values. All the required transition-rate expressions in intermediate coupling are presented.

I. INTRODUCTION

From the time of its first measurement the L_{23}-$M_{4,5}M_{4,5}$ Auger spectrum of Cu has attracted the interest of both experimentalists[1-6] and theorists.[7-9] One expected to see a spectrum characterized by a weighted self-fold of the density of states in Cu. Instead one found the Cu spectrum to be similar to that of Zn, Ga and Ge, i.e., atomiclike. The observed L_{23}-$M_{4,5}M_{4,5}$ spectrum is composed of several lines, separated in energy, with linewidths approximately equal to those obtained in an atomic calculation, and with an intensity pattern characteristic of the atom (the spectrum for solid Cu is similar to that of atomic Zn). An attempt to reproduce the Cu observations with a one-electron calculation using a calculated solid-state density of states[9] led to poor agreement. It also led to the hypothesis[5,10] that the crucial factor is the ratio of the two-electron correlation energy to the one-electron valence bandwidth. However, no calculations incorporating this hypothesis have yet been made.

Thus, from this point on, I assume the Cu spectrum can be treated as atomic. In the experiment of Antonides *et al.*[6] the Cu L_3/L_2 photoelectron intensity ratio was measured as 2.0, while the L_3-$M_{4,5}M_{4,5}/L_2$-$M_{4,5}M_{4,5}$ intensity ratio was measured as 5.3. This suggests[6,7] that L_2-L_3 Coster-Kronig transitions occur in solid Cu. A comparison of the solid and gaseous Zn $L_{2,3}$-$M_{4,5}M_{4,5}$ spectra[11] indicates that such Coster-Kronig processes occur in the solid but not in the gas. For Zn it is clear and for Cu it is strongly suggested that the L_2-L_3 Coster-Kronig transition is a solid-state effect. The question then arises: Is the spectrum arising from the L_2-L_3 Coster-Kronig transition similar to that for the atom or the solid? Roberts *et al.*[4] first pointed out that the Coster-Kronig transition leads to $L_3M_{4,5}$-$(M_{4,5})^3$ transitions and these should appear as satellite structure in the L_3-$(M_{4,5})^2$ spectrum. Antonides *et al.*[6] have extended this observation and attempted to draw quantitative conclusions from the satellite spectrum. In essence, their effort is a novel way to do experimental Coster-Kronig electron spectroscopy via satellite spectra, rather than do difficult, if not impossible, measurements on low-energy Coster-Kronig electrons. However a question that must be asked is, do the satellite spectra include effects other than the $L_3M_{4,5}$-$(M_{4,5})^3$ transitions arising from L_2-L_3 Coster-Kronig transitions? In particular, since L_1 vacancies decay via L_1-$L_2M_{4,5}$ and L_1-$L_3M_{4,5}$ Coster-Kronig transitions, then these will lead to satellite structure in both the L_2-$(M_{4,5})^2$ and L_3-$(M_{4,5})^2$ spectra. Without accounting for this effect the results of the experimental quantitative analysis are questionable.

This paper addresses itself to the question of satellite structure. I assume that the satellite spectra are atomiclike. From this assumption and standard techniques in atomic spectroscopy I will synthesize the spectra, including the results of L_1 Coster-Kronig decay, to compare with experiment. In Sec. II the necessary spectroscopic expressions are obtained, and in Sec. III the calculations are compared with experiment.

II. TRANSITION RATES

The transition rate expressions are obtained in intermediate coupling. They are presented in detail as they can be used for other elements, e.g., for the L_2-$L_3M_{4,5}$ spectra of the transuranic elements where persistent differences between measured and calculated $f_{2,3}$ values still exist.[12]

A. The Coster-Kronig transition

Since the initial holes are designated L_2 and L_3, for simplicity one wants to do the intermediate coupling calculations for the L_2-$L_3M_{4,5}$ Auger transition with j-j coupled wave functions. The necessary expressions in j-j coupling have been given by Asaad.[13] The intermediate coupling calculations should modify Asaad's results by the introduction of intermediate coupling coefficients. Since the phase factors are important I begin by using a general expression in mixed coupling for Auger transitions where the initial and one final-state hole are equivalent [Eq. (14) of Ref. 14]. For the case where the other final-state hole occurs in an initially filled shell, and one can neglect passive electron term structure, Eq. (14) of Ref. 14 reduces to

$$\frac{W_{if}}{2\pi} = (2j_2+1)(2P+1)(2Q+1)(2J+1)\prod_{i=1}^{4}(2l_i+1) \times \left| (-1)^{j_2-j_1+J+1-Q} \begin{Bmatrix} l_2 & \frac{1}{2} & j_2 \\ P & Q & J \\ l_1 & \frac{1}{2} & j_1 \end{Bmatrix} I'(KK'QP) \right|^2 \tag{1a}$$

where

$$I'(KK'QP) = \sum_K E(K) \begin{Bmatrix} l_1 & l_3 & K \\ l_1 & l_2 & P \end{Bmatrix} + (-1)^{Q-P} \times \sum_{K'} D(K') \begin{Bmatrix} l_1 & l_1 & K \\ l_3 & l_2 & P \end{Bmatrix},$$

where

$$E(K) = R_K(l_1l_2l_3l_1) \begin{pmatrix} l_1 & K & l_3 \\ 0 & 0 & 0 \end{pmatrix} \begin{pmatrix} l_2 & K & l_1 \\ 0 & 0 & 0 \end{pmatrix},$$

$$D(K) = R_K(l_1l_2l_1l_3) \begin{pmatrix} l_1 & K & l_1 \\ 0 & 0 & 0 \end{pmatrix} \begin{pmatrix} l_2 & K & l_3 \\ 0 & 0 & 0 \end{pmatrix},$$

$$R_K(l_1l_2l_3l_4) = \int d\vec{r}_1\, \phi_{l_1}(r_1)\phi_{l_3}(r_1) \times \int d\vec{r}_2\, \frac{(r_<)^K}{(r_>)^{K+1}}\, \phi_{l_2}(r_2)\phi_{l_4}(r_2), \tag{1b}$$

where l_1j_1, l_2j_2 are the quantum numbers of the initial vacancy and continuum hole, respectively, l_1, l_3 are quantum numbers of the final-state holes, and P, Q, J are the quantum numbers of the final-state ion. To transform Eq. (1) to one involving a final state in intermediate coupling based on j-j coupled wave functions we use

$$\phi_i(JM_J) = \sum_{j_1', j_3} C_i(j_1', j_3, J)\phi(j_1', j_3, J, M_J), \tag{2a}$$

where $\phi(j_1', j_3, J, M_J)$ is a two-electron wave function in j-j coupling, $\phi_i(JM_J)$ is a two-electron wave function in intermediate coupling, and $C_i(j_1', j_3, J)$ is an intermediate-coupling mixing parameter and

$$\phi(j_1', j_3, JM_J) = \sum_{PQ} [(2j_3+1)(2j_1'+1) \times (2P+1)(2Q+1)]^{1/2} \times \begin{Bmatrix} \frac{1}{2} & \frac{1}{2} & Q \\ l_3 & l_1 & P \\ j_3 & j_1' & J \end{Bmatrix} \Phi(PQJM_J). \tag{2b}$$

Since Eq. (1) is obtained with a final-state wave function of the form $\Phi(PQJM_J)$, the result we desire, in intermediate coupling is

$$\frac{W_{if}}{2\pi} = (2j_2+1)(2J+1)(2l_1+1)^2(2l_2+1)(2l_3+1) \times \left| \sum_{j_1', j_3} C_i(j_1', j_3, J)(-1)^{j_2-j_1+J} \sum_{PQ} (-1)^Q (2P+1)(2Q+1)[(2j_1'+1)(2j_3+1)]^{1/2} \times \begin{Bmatrix} \frac{1}{2} & \frac{1}{2} & Q \\ l_3 & l_1 & P \\ j_3 & j_1' & J \end{Bmatrix} \begin{Bmatrix} \frac{1}{2} & \frac{1}{2} & Q \\ l_2 & l_1 & P \\ j_2 & j_1 & J \end{Bmatrix} I'(KK'QP) \right|^2. \tag{3}$$

Manipulation of the 6-j and 9-j symbols in Eq. (3) leads to the desired result (the modification of Asaad's result[13]):

$$\frac{W_{if}(i,J)}{2\pi} = (2J+1)(2l_1+1)^2(2l_3+1)\sum_{l_2,j_2}(2l_2+1)(2j_2+1)$$

$$\times\Bigg|\sum_{j_1',j_3}(-1)^{j_1-j_3}C_i(j_1',j_3,J)[(2j_1'+1)(2j_3+1)]^{1/2}$$

$$\times\sum_K\Bigg[D(K,l_2)\begin{pmatrix}l_1 & K & l_1\\ 0 & 0 & 0\end{pmatrix}\begin{pmatrix}l_2 & K & l_3\\ 0 & 0 & 0\end{pmatrix}\begin{Bmatrix}j_3 & j_1' & J\\ j_1 & j_2 & K\end{Bmatrix}\begin{Bmatrix}\frac{1}{2} & l_1 & j_1'\\ K & j_1 & l_1\end{Bmatrix}\begin{Bmatrix}\frac{1}{2} & l_3 & j_3\\ K & j_2 & l_2\end{Bmatrix}$$

$$+(-1)^J\sum_K E(K,l_2)\begin{pmatrix}l_1 & K & l_3\\ 0 & 0 & 0\end{pmatrix}\begin{pmatrix}l_2 & K & l_1\\ 0 & 0 & 0\end{pmatrix}\begin{Bmatrix}j_3 & j_1' & J\\ j_2 & j_1 & K\end{Bmatrix}\begin{Bmatrix}\frac{1}{2} & l_1 & j_1'\\ K & j_2 & l_2\end{Bmatrix}\begin{Bmatrix}\frac{1}{2} & l_3 & j_3\\ K & j_1 & l_1\end{Bmatrix}\Bigg]\Bigg|^2 , \tag{4}$$

where $D(K,l_2)=R_K(l_1l_2l_1l_3)$ and $E(K,l_2)=R_K(l_1l_2l_3l_1)$, and (i,J) are eigenfunction labels in intermediate coupling.

Explicit expressions for $W_{if}(i,J)/2\pi$ for $l_1=1$ and $l_3=2$ are given in Table I. To determine the relative energy positions of the $L_3M_{4,5}$ terms in intermediate coupling using j-j coupled wave functions requires we determine matrix elements of the electrostatic interaction. The matrix element is

$$M=[(2j_1'+1)(2j_3+1)(2j_1''+1)(2j_3'+1)]^{1/2}$$

$$\times\sum_{LS}(2L+1)(2S+1)E(LS)\begin{Bmatrix}2 & 1 & L\\ j_3 & j_1' & J\\ \frac{1}{2} & \frac{1}{2} & S\end{Bmatrix}\begin{Bmatrix}2 & 1 & L\\ j_3' & j_1'' & J\\ \frac{1}{2} & \frac{1}{2} & S\end{Bmatrix}, \tag{5}$$

where $E(LS)$ is the term splitting in LS coupling. $E(LS)$ was determined via expressions in Slater[15] and Mann's[16] electrostatic integrals. The diagonal spin-orbit terms were obtained from the experimental L_2-L_3 splitting of 20 eV. The relative energies of the $L_{2,3}M_{4,5}$ terms are shown on the left-hand side of Fig. 1. The lower set of levels for $L_3M_{4,5}$ terms are the only important ones in the L_2-L_3 Coster-Kronig transitions. The splitting of the lower terms is 3.3 eV. In j-j coupling, neglecting the $3d$ spin-orbit parameter, all the lower levels would be degenerate with relative energy of −6.67 eV. On the right-hand side of Fig. 1 the relative term splittings of the $(3d)^7$ configuration are shown. They are found using Slater's[15] expressions and Mann's[16] tables. The L_3-$M_{4,5}M_{4,5}$ satellite spectrum arising from the L_2-$L_3M_{4,5}$ Coster-Kronig transition is between terms on the lower left and those on the right. The rates for such transitions are determined next.

B. The satellite spectrum

To calculate the $L_3M_{4,5}$-$(M_{4,5})^3$ satellite spectrum one requires detailed transition rates between the terms (i,J), and the terms P_3Q_3 of the $(3d)^7$ configuration. For the $(3d)^7$ configuration spin-orbit interaction is neglected, and the nondiagonal matrix element between ^2D terms of $(3d)^7$ is neglected (transitions to the ^2D terms are weak). In determining the widths of the (i,J) terms, one sums over P_3 and Q_3.

It is shown in the Appendix that the transition rate for $L_{2,3}(M_{4,5})^n \rightarrow (M_{4,5})^{n+2}$ is given by

$$\frac{W_{if}(iJ,P_3Q_3)}{2\pi} = \sum_{LS}(2L+1)(2S+1)\frac{W_{if}(LS,P_3Q_3)}{2\pi}$$

$$\times\Bigg|\sum_{j_1',J_3}C_i(j_1'J_3J)[(2j_1'+1)(2J_3+1)]^{1/2}\begin{Bmatrix}S_3 & \frac{1}{2} & S\\ L_3 & l_1 & L\\ J_3 & j_1' & J\end{Bmatrix}\Bigg|^2 , \tag{6}$$

where $W_{if}(LS,P_3Q_3)/2\pi$ is the multiplet transition rate.[17] Explicit expressions for $W_{if}(LS,P_3Q_3)/2\pi$ for $L_{2,3}M_{4,5}$-$(M_{4,5})^3$ are given in Table II.

To compute the contribution of transitions of the form $(p)^5(s)^2(d)^9 \rightarrow (p)^6(s)^1(d)^8$ and $(p)^5(p')^6(d)^9 \rightarrow (p)^6(p')^5(d)^8$ to the width of the i,J terms we use

TABLE I. Auger transition rate (in atomic units) in intermediate coupling for L_2-$L_3M_{4,5}$.

Final-state term J, i	$W_{if}(iJ)/2\pi$
$4a$	$\frac{81}{14}[\frac{1}{5}D(2,4)-\frac{1}{7}E(3,4)]^2$
$3i$	$\frac{7}{2}\lvert C_i(\frac{1}{2},\frac{5}{2},3)[D(0,2)-\frac{1}{49}E(3,2)]+(\frac{6}{5})^{1/2}C_i(\frac{3}{2},\frac{3}{2},3)[\frac{1}{35}D(2,2)-\frac{1}{3}E(1,2)]-(4/7\sqrt{5})C_i(\frac{3}{2},\frac{5}{2},3)[\frac{2}{5}D(2,2)+\frac{1}{7}E(3,2)]\rvert^2$
	$+\frac{144}{875}\lvert-(25/7\sqrt{30})C_i(\frac{1}{2},\frac{5}{2},3)E(3,4)+C_i(\frac{3}{2},\frac{3}{2},3)D(2,4)+(15/4\sqrt{6})C_i(\frac{3}{2},\frac{5}{2},3)[\frac{1}{5}D(2,4)+\frac{5}{21}E(3,4)]\rvert^2$
$2i$	$\frac{5}{2}\lvert-C_i(\frac{1}{2},\frac{3}{2},2)[D(0,2)-\frac{1}{3}E(1,2)]+\frac{2}{5}C(\frac{3}{2},\frac{3}{2},2)[\frac{1}{5}D(2,2)-\frac{1}{3}E(1,2)]+\frac{3}{5}(\frac{3}{7})^{1/2}C_i(\frac{3}{2},\frac{5}{2},2)[\frac{1}{5}D(2,2)-\frac{1}{7}E(3,2)]\rvert^2$
	$+\frac{5}{2}\lvert-C_i(\frac{1}{2},\frac{5}{2},2)[D(0,2)-\frac{1}{7}E(3,2)]+\frac{1}{5}\sqrt{6}C_i(\frac{3}{2},\frac{3}{2},2)[\frac{1}{5}D(2,2)-\frac{1}{3}E(1,2)]$
	$+(16/5\sqrt{14})C_i(\frac{3}{2},\frac{5}{2},2)[\frac{1}{5}D(2,2)-\frac{1}{7}E(3,2)]\rvert^2$
$1i$	$\frac{4}{27}\lvert-C_i(\frac{1}{2},\frac{3}{2},1)E(1,0)+(9/2\sqrt{5})C_i(\frac{3}{2},\frac{3}{2},1)[\frac{1}{5}D(2,0)-\frac{5}{9}E(1,0)]-(9/5\sqrt{5})C_i(\frac{3}{2},\frac{5}{2},1)D(2,0)\rvert^2$
	$+\frac{3}{2}\lvert C_i(\frac{1}{2},\frac{3}{2},1)[D(0,2)+\frac{1}{9}E(1,2)]$
	$+(2/\sqrt{5})C_i(\frac{3}{2},\frac{3}{2},1)[\frac{1}{5}D(2,2)-\frac{1}{9}E(1,2)]+(1/\sqrt{5})C_i(\frac{3}{2},\frac{5}{2},1)[\frac{1}{5}D(2,2)+\frac{1}{7}3E(3,2)]\rvert^2$
$0a$	$[\frac{1}{5}D(2,0)-\frac{1}{3}E(1,0)]^2$

$$\sum_{PQ}\frac{W_{if}(iJ,PQ)}{2\pi}=\sum_{LS,\,PQ}(2L+1)(2S+1)\frac{W_{if}(LS,PQ)}{2\pi}\left|\sum_{j_1'j_3}C_i(j_1'j_3J)[(2j_1'+1)(2j_3+)]^{1/2}\begin{Bmatrix}\frac{1}{2} & \frac{1}{2} & S\\ l_3 & l_1 & L\\ j_3 & j_1' & J\end{Bmatrix}\right|^2. \tag{7}$$

Explicit expressions for $\sum_{PQ}W_{if}(LS,PQ)/2\pi$ for $(2p)^5(3s)^2(3d)^n \rightarrow (2p)^6(3s)(3d)^{n-1}$ are found in Ref. 17. For $(2p)^5(3p)^6(3d)^9 \rightarrow (2p)^6(3p)^5(3d)^8$ explicit expressions are given in Table III.

Finally, as the satellite spectrum arising from the Auger decay of L_1 holes is included in the calculation, expressions for the transition rates are given in Table IV.

III. THE CALCULATIONS

For Mg K_α radiation incident of Cu, Zn, and Ga, I use tabulated[18] subshell photoionization cross sections to determine initial $L_1:L_2:L_3$ vacancy ratios of 26:54:100, 19:53:100, and 0:53:100, for Cu, Zn, and Ga, respectively. The $L_{2,3}$-$M_{4,5}M_{4,5}$ Auger transition rate expressions were evaluated using tabulated[19] values. These calculations[19] were done with an approximation[20] to the central potential of Herman and Skillman[21] for an atom with a $2p$ hole. In addition new calculations were performed with the neutral-atom central potential. Yin *et al.*[8] have pointed out that near $Z=30$, calculated M-shell transition rates can vary significantly if one used the neutral-atom potential rather than the potential for the ion with an M-shell hole. In addition experiment[8] favors the neutral-atom potential. This effect also occurs in the L-shell transition rates. In Table V I compare my calculated transition rates for the ion with an L-shell hole with those calculated by Walters and Bhalla[22] for a neutral-atom potential. As can be seen in Table V the significant differences in the two calculations are transitions involving $3d$ electrons. The $3d$ orbitals are most affected by the difference in potential. With the rates of Ref. 19 and Ref. 22 the ratio of L_{23}-$M_{2,3}M_{2,3}$: L_{23}-$M_{2,3}M_{4,5}$: L_{23}-$M_{4,5}M_{4,5}$ intensities in Zn are 22:34:43 and 26:34:40, respectively. Aksela and Aksela[23] measure a ratio of 14:30:56. It is possible that the difference between the calculations and measurement is the neglect of configuration interaction between the ^1S, ^3P, and ^1D terms of $(M_{2,3})^2$ and $(M_{4,5})^2$. In any case the measurements of Aksela and Aksela do not distinguish between the two calculations.

For Cu my calculations with the ion potential indicate that L_2-$L_3M_{4,5}$ transitions contribute a width of 0.34 eV. Thus with the ion potential[19] one has $\Gamma(L_2)=1.10$ eV and $\Gamma(L_3)=0.76$ eV. With the neutral-atom potential[22] one has $\Gamma(L_2)=0.93$

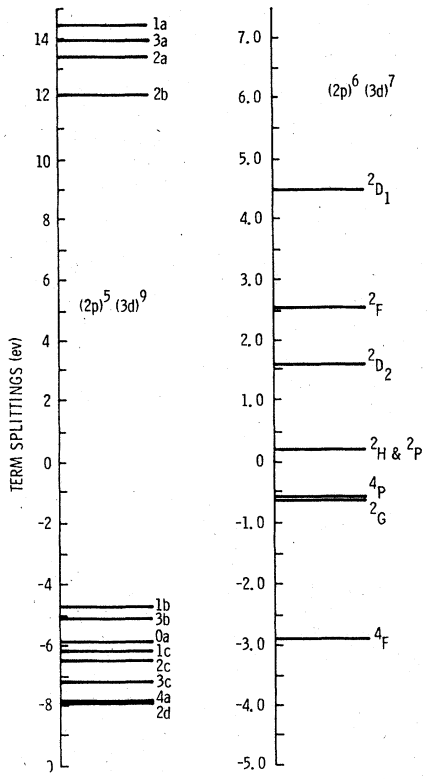

FIG. 1. Relative energy of i,J terms of $(2p)^5(3d)^9$ and of P_3Q_3 terms of $(2p)^6(3d)^7$.

eV and $\Gamma(L_3)=0.59$ eV. Yin *et al.*[7] report measured values of $\Gamma(L_2)=0.98\pm0.04$ and $\Gamma(L_3)=0.54\pm0.03$ eV. The measurements clearly support $L_{2,3}$ Auger-rate calculations with the neutral-atom potential. However the Coster-Kronig width (0.34 eV) was obtained[19] with the ion potential. While it is difficult to understand why neutral-atom wave functions are to be preferred in transitions from single- to double-charged ions, it is even more difficult to justify neutral-atom wave functions in the satellite spectra, double- to triple-charged ions. To cover both cases I have computed the relevant Cu matrix elements with a neutral-atom potential. The matrix elements are listed in Table VI, with the neutral-atom values listed first.[24] For the L_2-$L_3M_{4,5}$ transition matrix elements were calculated at Auger electron energies of 5 and 10 eV. No significant change in matrix element was found. The striking feature is the change in $E(1,2)$ in both the L_2-$L_3M_{4,5}$ and L_{23}-$M_{23}M_{45}$ transitions. With the neutral-atom potential the L_{23}-$M_{2,3}M_{4,5}$ and L_{23}-$(M_{4,5})^2$ rates are 51.1 and 60.9, somewhat lower than the values calculated by Walters and Bhalla.[22] The calculated width is $\Gamma(L_3)=0.50$ eV.

It is suggested by Table V that the satellite spectra for Cu and Zn should be similar, when matrix elements are calculated with the ion potential. The Coster-Kronig matrix elements are also similar, reinforcing the suggestion. But the measurements[4-8] indicate that the spectra are significantly different in the two cases! How can this occur? Yin *et al.*[7] suggest that the difference can occur because L_2-L_3M_4 transitions are energetically forbidden while L_2-L_3M_5 transitions are allowed in Zn, while both transitions are allowed in Cu.

My calculations indicate that the difference occurs as an effect of spin-orbit interaction and the choice of potentials, and only appears when the L_2-L_3 Coster-Kronig rate is calculated in intermediate coupling. That is, in intermediate coupling for the ion potential, transitions to $L_3M_{4,5}$ terms with $J=3$ are almost eliminated. In j-j coupling, using Asaad's[13] expressions I find transition rates of 276, 25, and 112 for $J=3$, 2, and 1, respectively. In intermediate coupling the rates are 9.0, 97.5, and 9.9, for $J=3$, 2, and 1 respectively. With the neutral-atom potential and intermediate coupling the rates are 283, 196, and 26.2, for $J=3$, 2, and 1, respectively. To see how this occurs I list the configuration interaction mixing parameters for $J=3$ in Table VII.

In Table VIII I list the initial populations in $L_3M_{4,5}$ terms as a result of the L_2 Coster-Kronig transition. For consistency sake I use the L_{23}-MM rates calculated with the ion potential. Also listed are the initial populations in $L_{2,3}M_{4,5}$ terms due to L_1 Coster-Kronig transitions.

With the neutral-atom potential I calculate $\Gamma_{CK}(L_2)=1.37$ eV and $f_{2,3}=0.64$ (with $f_{2,3}=\Gamma_{CK}(L_2)/[\Gamma_A+\Gamma_{CK}(L_2)]$, and $\Gamma_A=0.76$ eV. With the ion potential I calculate $\Gamma_{CK}(L_2)=0.34$ eV and $f_{2,3}=0.31$, with $\Gamma_A=0.76$ eV. With the neutral-atom potential the calculated $\Gamma_{CK}(L_2)$ is considerably larger than the measured[7] $\Gamma(L_2)$. In their calculations based on a neutral atom potential but neglecting spin-orbit effects Yin *et al.*[7] find $\Gamma_{CK}(L_2)=0.92$ eV and $f_{2,3}=0.64$ for Cu, but the authors point out that the calculated width is considerably in excess of the measured L_2 width.

With these two quite different L_2 Coster-Kronig transition-rate calculations I have synthesized the $L_{2,3}$ spectra. One other table is necessary: the transition rates from the i,J terms of $(2p)^5(3d)^9$ to the terms of $(2p)^6(3d)^7$. These rates, the total transition rates of i,J terms, relative energies, and the calculated widths are given in Table IX. With Table IX and the initial populations one can synthesize the spectra. In Table IX, it is clear that while the ^{2}H term of $(3d)^7$ stands out as the most important final-state term, it does not dominate the decay of the i,J levels of $(2p)^5(3d)^9$, and

TABLE II. Multiplet transition rates for $(2p)^5(3d)^9\ LS \rightarrow (2p)^6(3d)^7\ P_3Q_3$.

P_3Q_3 \ LS	$W_{if}(LS, P_3Q_3)$ for $(p)^5(d)^9 \rightarrow (d)^7$
	^3F
^4F	$\frac{16}{75}[D(1,1)-\frac{3}{7}D(3,1)]^2+\frac{32}{175}[D(1,3)-\frac{3}{7}D(3,3)]^2$
^4P	$[16/25(63)][D(1,3)-\frac{3}{7}D(3,3)]^2$
^2H	$\frac{22}{245}[D(1,3)+\frac{2}{7}D(3,3)]^2+\frac{13}{345}D(3,5)^2$
^2G	$\frac{3}{35}[D(1,1)+\frac{9}{49}D(3,1)]^2+\frac{22}{245}[D(1,3)-\frac{3}{7}D(3,3)]^2+[13(36)/49(343)]D(3,5)^2$
^2F	$\frac{1}{75}[D(1,1)-\frac{51}{49}D(3,1)]^2+\frac{2}{175}[D(1,3)+D(3,3)]^2+[100/49(49)]D(3,5)^2$
$^2D_1$	$\frac{4}{225}[D(1,1)+\frac{153}{98}D(3,1)]^2+\frac{3}{175}[D(1,3)+\frac{2}{7}D(3,3)]^2+[75/49(98)]D(3,5)^2$
$^2D_2$	$\frac{4}{525}[D(1,1)-\frac{87}{98}D(3,1)]^2+[9/25(49)][D(1,3)+\frac{26}{21}D(3,3)]^2+[625/98(343)]D(3,5)^2$
^2P	$[32/49(225)][D(1,3)+\frac{39}{14}D(3,3)]^2$
	^1F
^4F	0
^4P	0
^2H	$\frac{198}{245}[D(1,3)-\frac{4}{21}D(3,3)]^2+\frac{13}{343}D(3,5)^2$
^2G	$\frac{3}{35}[D(1,1)+\frac{9}{49}D(3,1)]^2+\frac{22}{245}[D(1,3)-\frac{3}{7}D(3,3)]^2+[13(36)/49(343)]D(3,5)^2$
^2F	$\frac{49}{75}[D(1,1)-\frac{117}{343}D(3,1)]^2+\frac{18}{175}[D(1,3)+\frac{1}{21}D(3,3)]^2+[100/49(49)]D(3,5)^2$
$^2D_1$	$\frac{64}{225}[D(1,1)+\frac{27}{392}D(3,1)]^2+\frac{3}{175}[D(1,3)-\frac{8}{7}D(3,3)]^2+[75/49(98)]D(3,5)^2$
$^2D_2$	$\frac{48}{175}[D(1,1)-\frac{69}{196}D(3,1)]^2+[9/25(49)][D(1,3)-\frac{44}{21}D(3,3)]^2+[625/98(343)]D(3,5)^2$
^2P	$[32/25(49)][D(1,3)+\frac{9}{14}D(3,3)]^2$
	^3D
^4F	$\frac{56}{375}[D(1,1)-\frac{3}{7}D(3,1)]^2+\frac{8}{125}[D(1,3)-\frac{3}{7}D(3,3)]^2$
^4P	$\frac{48}{125}[D(1,1)-\frac{3}{7}D(3,1)]^2+\frac{128}{1125}[D(1,3)-\frac{3}{7}D(3,3)]^2$
^2H	$\frac{88}{175}[D(1,3)-\frac{1}{14}D(3,3)]^2+\frac{26}{343}D(3,5)^2$
^2G	$\frac{32}{175}[D(1,3)+\frac{3}{8}D(3,3)]^2+\frac{9}{343}D(3,5)^2$
^2F	$\frac{56}{375}[D(1,1)-\frac{6}{49}D(3,1)]^2+\frac{8}{125}[D(1,3)-\frac{1}{4}D(3,3)]^2+\frac{5}{343}D(3,5)^2$
$^2D_1$	$\frac{169}{900}[D(1,1)+\frac{36}{91}D(3,1)]^2+\frac{1}{25}[D(1,3)-\frac{3}{7}D(3,3)]^2$
$^2D_2$	$\frac{7}{300}[D(1,1)+\frac{24}{49}D(3,1)]^2+\frac{3}{175}[D(1,3)+D(3,3)]^2$
^2P	$\frac{21}{250}[D(1,1)-\frac{6}{49}D(3,1)]^2+[121/35(225)][D(1,3)+\frac{12}{77}D(3,3)]^2$
	^1D
^4F	0
^4P	0
^2H	$\frac{22}{343}D(3,3)^2+\frac{26}{343}D(3,5)^2$
^2G	$\frac{2}{7}[D(1,3)+\frac{3}{14}D(3,3)]^2+\frac{9}{343}D(3,5)^2$
^2F	$\frac{56}{375}[D(1,1)-\frac{36}{49}D(3,1)]^2+\frac{18}{125}[D(1,3)-\frac{13}{42}D(3,3)]^2+\frac{5}{343}D(3,5)^2$
$^2D_1$	$\frac{49}{900}[D(1,1)+\frac{54}{49}D(3,1)]^2+\frac{1}{25}[D(1,3)-\frac{3}{7}D(3,3)]^2$
$^2D_2$	$\frac{21}{100}[D(1,1)-\frac{6}{49}D(3,1)]^2+\frac{27}{175}[D(1,3)+\frac{1}{21}D(3,3)]^2$
^2P	$\frac{21}{250}[D(1,1)-\frac{36}{49}D(3,1)]^2+\frac{7}{125}[D(1,3)-\frac{36}{49}D(3,3)]^2$

TABLE II. (*Continued*)

P_3Q_3 \ LS	$W_{if}(LS, P_3Q_3)$ for $(p)^5(d)^9 \rightarrow (d)^7$
	^3P
^4F	$\frac{8}{25}[D(1,3) - \frac{3}{7}D(3,3)]^2$
^4P	$\frac{16}{75}[D(1,1) - \frac{3}{7}D(3,1)]^2$
^2H	$\frac{18}{343}D(3,5)^2$
^2G	$\frac{5}{686}D(3,3)^2 + \frac{2}{343}D(3,5)^2$
^2F	$\frac{8}{25}[D(1,3) + \frac{3}{28}D(3,3)]^2$
$^2D_1$	$\frac{9}{100}[D(1,1) + \frac{2}{7}D(3,1)]^2 + \frac{3}{50}[D(1,3) + \frac{2}{7}D(3,3)]^2$
$^2D_2$	$\frac{21}{100}[D(1,1) - \frac{6}{49}D(3,1)]^2 + \frac{7}{50}[D(1,3) - \frac{6}{49}D(3,3)]^2$
^2P	$\frac{7}{150}[D(1,1) + \frac{24}{49}D(3,1)]^2$
	^1P
^4F	0
^4P	0
^2H	$\frac{18}{343}D(3,5)^2$
^2G	$\frac{18}{35}[D(1,3) - \frac{23}{42}D(3,3)]^2 + \frac{2}{343}D(3,5)^2$
^2F	$\frac{2}{25}[D(1,3) + \frac{9}{14}D(3,3)]^2$
$^2D_1$	$\frac{9}{100}[D(1,1) - \frac{8}{7}D(3,1)]^2 + \frac{49}{150}[D(1,3) - \frac{6}{49}D(3,3)]^2$
$^2D_2$	$\frac{21}{100}[D(1,1) - \frac{36}{49}D(3,1)]^2 + \frac{9}{350}[D(1,3) + \frac{2}{7}D(3,3)]^2$
^2P	$\frac{21}{50}[D(1,1) - \frac{6}{49}D(3,1)]^2$

TABLE III. Multiplet transition rate for $(2p)^5(3p)^6(3d)^9\ LS \rightarrow (2p)^6(3p)^5(3d)^8\ PQ$ summed over PQ.

LS	$\sum_{PQ} W(LS, PQ)/2\pi$ for $(p)^5(p')^6(d)^9 \rightarrow (p)^6(p')^5(d)^8$
^3F	$126U_1 + 36U_2 + 3U_3 + 396U_4 + 204U_5$
^1F	$126U_1 + 144U_2 + 3U_3 + 396U_4 + 216U_5$
^3D	$207U_1 + 117U_2 + \frac{5}{2}U_3 + 378U_4 + 168U_5$
^1D	$207U_1 + 63U_2 + \frac{5}{2}U_3 + 378U_4 + 252U_5$
^3P	$171U_1 + 81U_2 + \frac{23}{6}U_3 + 294U_4 + 84U_5$
^1P	$171U_1 + 99U_2 + \frac{23}{6}U_3 + 294U_4 + 336U_5$

where

$$U_1 = D(2,0)^2/9(125) + \tfrac{1}{90}[D(0,2) + \tfrac{1}{5}D(2,2)]^2,$$

$$U_2 = \tfrac{2}{45}E(1,0)[\tfrac{1}{9}E(1,0) - \tfrac{1}{15}D(2,0)] + \tfrac{2}{9}E(1,2)[\tfrac{2}{45}E(1,2) - \tfrac{1}{15}D(0,2) - \tfrac{1}{75}D(2,2)],$$

$$U_3 = [D(0,2) - \tfrac{1}{5}D(2,2)]^2,$$

$$U_4 = \tfrac{1}{90}[D(0,2) + \tfrac{2}{35}D(2,2)]^2 + [6/49(125)]D(2,4)^2,$$

$$U_5 = \tfrac{3}{49}E(3,2)[\tfrac{3}{245}E(3,2) - \tfrac{1}{15}D(0,2) - [2/15(35)]D(2,2)] + \tfrac{18}{245}E(3,4)[\tfrac{2}{147}E(3,4) - \tfrac{2}{105}D(2,4)].$$

TABLE IV. Auger transition rate (in atomic units) in intermediate coupling for L_1-$L_{2,3}M_{4,5}$.

Final-state term J, i	$W_{if}(iJ)/2\pi$
$4a$	$\frac{81}{14}[\frac{1}{3}D(1,3)-\frac{1}{5}E(2,3)]^2$
$3i$	$189\lvert[C_i(\frac{1}{2},\frac{5}{2},3)/3\sqrt{6}][\frac{1}{21}D(1,3)-\frac{1}{5}E(2,3)]+[C_i(\frac{3}{2},\frac{3}{2},3)/3\sqrt{5}][\frac{1}{3}D(1,3)-\frac{1}{35}E(2,3)]$ $+\frac{2}{63}(\frac{6}{5})^{1/2}C_i(\frac{3}{2},\frac{5}{2},3)[\frac{1}{3}D(1,3)+\frac{2}{5}E(2,3)]\rvert^2+252\lvert\frac{1}{63}\sqrt{6}\,C_i(\frac{1}{2},\frac{5}{2},3)D(1,3)-(2/35\sqrt{5})C_i(\frac{3}{2},\frac{3}{2},3)E(2,3)$ $-\frac{1}{84}(\frac{6}{5})^{1/2}C_i(\frac{3}{2},\frac{5}{2},3)[\frac{5}{3}D(1,3)+\frac{3}{5}E(2,3)]\rvert^2$
$2i$	$60\lvert-[C_i(\frac{1}{2},\frac{3}{2},2)/10\sqrt{6}][\frac{1}{3}D(1,1)-\frac{1}{5}E(2,1)]+\frac{1}{5}C_i(\frac{1}{2},\frac{5}{2},2)[\frac{1}{3}D(1,1)-\frac{1}{5}E(2,1)]-[C_i(\frac{3}{2},\frac{3}{2},2)/5\sqrt{6}][\frac{1}{3}D(1,1)$ $-\frac{1}{5}E(2,1)]+(7/5\sqrt{56})C_i(\frac{3}{2},\frac{5}{2},2)[\frac{1}{3}D(1,1)-\frac{1}{5}E(2,1)]\rvert^2+135\lvert\frac{2}{15}C_i(\frac{1}{2},\frac{3}{2},2)[\frac{1}{3}D(1,3)-\frac{1}{5}E(2,3)]$ $+[C_i(\frac{1}{2},\frac{5}{2},2)/15\sqrt{6}][\frac{1}{3}D(1,3)-\frac{1}{5}E(2,3)]-\frac{1}{15}C_i(\frac{3}{2},\frac{3}{2},2)[\frac{1}{3}D(1,3)-\frac{1}{5}E(2,3)]$ $-(2/15\sqrt{21})C_i(\frac{3}{2},\frac{5}{2},2)[\frac{1}{3}D(1,3)-\frac{1}{5}E(2,3)]\rvert^2$
$1i$	$18\lvert C_i(\frac{1}{2},\frac{3}{2},1)(2/9\sqrt{6})D(1,1)+[C_i(\frac{3}{2},\frac{3}{2},1)/3\sqrt{30}][\frac{5}{3}D(1,1)-\frac{3}{5}E(2,1)]+\frac{1}{5}(\frac{2}{15})^{1/2}C_i(\frac{3}{2},\frac{5}{2},1)E(2,1)\rvert^2$ $+36\lvert[C_i(\frac{1}{2},\frac{3}{2},1)/6\sqrt{6}]$ $\times[\frac{1}{3}D(1,1)+\frac{3}{5}E(2,1)]-[C_i(\frac{3}{2},\frac{3}{2},1)/3\sqrt{30}][\frac{1}{3}D(1,1)-\frac{3}{5}E(2,1)]+\frac{1}{4}(\frac{6}{5})^{1/2}C_i(\frac{3}{2},\frac{5}{2},1)[\frac{1}{3}D(1,1)+\frac{1}{15}D(2,1)]\rvert^2$
$0a$	$[\frac{1}{3}D(1,1)-\frac{1}{5}E(2,1)]^2$

as a result one expects the satellite spectrum will be a superposition of many transitions.

In Fig. 2 I show the synthesized Cu $L_{2,3}$ spectra, using transition rates calculated with the ion potential. I assume the detector response is rectangular in energy with a width of 0.25 eV. The figures on the left show the L_3 satellite spectra arising from the L_2-L_3M_{45} Coster-Kronig transition, the L_1-$L_3M_{4,5}$ Coster-Kronig transition, and the sum of the two. The numbers above the sum indicate how the satellite spectra was oriented relative to the principal spectra abscissa for addition. At this point the orientation is somewhat arbitrary.

By expanding and contracting the energy scale, Antonides *et al.*[6] have superimposed their Cu, Zn, and Ga spectra. Their superimposed data are compared with the synthesized spectra in Fig. 2. The calculated spectrum is spread over too broad an energy range as compared with the measurements of Roberts *et al.*[4] (A–E in Fig. 2). Except for this scale expansion, the synthesized spectrum, labeled a, is in excellent agreement with the Ga measurements of Antonides *et al.*[6] (the data points are not shown). Further, except for the scale expansion the synthesized spectrum, labeled b, is in excellent agreement with the measurement of Antonides *et al.*[6] on Zn (the crosses in Fig. 2). This latter result, which at first may appear surprising since I am attempting to synthesize the Cu spectrum, is not so for two reasons. First, Antonides *et al.* have effectively scaled the Zn spectrum to a Cu energy scale. Second, little difference was found between the Cu and Zn Auger matrix elements when the ion potential was used.

Two strong conclusions emerge from Fig. 2. First, the Zn L_2-$M_{4,5}M_{4,5}$ satellite spectrum contains a significant contribution from L_1 decay,

TABLE V. Calculation of Cu and Zn L_3-MM Auger transition rates using a potential with a $2p$ hole (first entry) and a neutral-atom potential (second entry).

Calculation	Element	$(3s)^2$	$(3s)(3p)$	$(3s)(3d)$	$(3p)^2$	$(3p)(3d)$	$(3d)^2$	Γ_{L_3} (eV)
Ref. 21	Cu	0.92	15.8	2.3	64.8	87.1	108	0.76
Ref. 22		0.81	15.3	2.2	56.1	68.9	74.4	0.59
Ref. 21	Zn	0.89	15.2	3.1	57.9	90.4	113	0.76
Ref. 22		0.82	15.7	2.4	58.0	77.0	90.0	0.66

TABLE VI. Comparison of calculated Cu L_2 Auger matrix elements. The first entry used a neutral-atom potential, and the second used a potential for an ion with a $2p$ hole.

L_2-$L_3M_{4,5}$								$(3s)^2$
$E(1,0)$	$D(2,0)$	$D(2,4)$	$E(3,4)$	$D(0,2)$	$D(2,2)$	$E(1,2)$	$E(3,2)$	$D(1,1)$
1.07	1.44	0.0226	0.0005	25.72	7.69	13.42	3.55	0.775
1.21	1.45	0.0030	0.0142	22.00	8.07	6.95	3.99	0.810

$3s$-$3p$				$3s$-$3d$			
$E(0,0)$	$D(1,0)$	$D(1,2)$	$E(2,2)$	$D(1,1)$	$E(1,1)$	$D(1,3)$	$E(3,3)$
0.858	0.765	−0.092	0.055	0.081	−0.313	0.109	1.04
0.890	0.810	0.113	0.050	0.080	−0.415	0.110	1.22

$(3p)^2$			$(3p)(3d)$							
$D(2,3)$	$D(0,1)$	$D(2,1)$	$E(1,0)$	$D(2,0)$	$D(2,4)$	$E(3,4)$	$D(0,2)$	$D(2,2)$	$E(1,2)$	$E(3,2)$
0.934	0.947	0.675	−0.790	−0.299	−1.07	−1.39	0.623	0.648	0.743	0.700
1.03	1.02	0.700	−1.01	−0.400	−1.27	−1.65	0.750	0.750	1.72	0.810

$(3d)^2$				
$D(3,5)$	$D(1,1)$	$D(3,1)$	$D(1,3)$	$D(3,3)$
0.929	−0.601	−0.501	2.31	1.47
1.13	−0.830	−0.690	3.08	1.95

and this must be subtracted out before any attempt can be made to identify the satellite spectra with L_2-$L_3M_{4,5}$ Auger transitions. Second, the ion potential does not reproduce the Cu satellite spectrum, the open circles in Fig. 2.

The decay of L_1 vacancies via $L_{2,3}M$ Coster-Kronig transitions leads to an L_2-$M_{4,5}M_{4,5}$ satellite spectrum. Once the L_3 satellite spectra have been located, the position of the L_2 satellite spectra is fixed. In Fig. 2 the L_2 spectra are shown on the right-hand side. The peak labeled G was located 20 eV above the peak D, i.e., these peaks are mostly due to Auger transitions to the ^1G term of $(3d)^8$. Roberts *et al.*[4] observe the peak G but not H in the Cu spectrum, but they do observe an additional peak at F. I assume that in the Cu measurements peaks G and H are considerably weaker than in the calculations in Fig. 2 so that H is not observed, and that peak F is the $L_2M_{4,5}$-$(M_{4,5})^3$ transition arising from the L_1-$L_2M_{4,5}$ Coster-Kronig transition. In Fig. 2 I label the L_2 principal spectrum as c, and with the added satellite as d. The energy shift between F and F' is 2 eV. Since the zero of energy in Fig. 2 is peak (D), peak F' is about 20 eV from the zero, and the difference between F and F' is 2 eV in 20 eV, comparable to the percentage difference between calculation

TABLE VII. Intermediate coupling mixing parameters for the $J=3$ terms of Cu$(2p)^5(3d)^9$.

IC	Terms		
	$\frac{1}{2},\frac{5}{2},3$	$\frac{3}{2},\frac{3}{2},3$	$\frac{3}{2},\frac{5}{2},3$
$3a$	0.9955	−0.0831	−0.0449
$3b$	0.0889	0.6635	−0.7428
$3c$	−0.0319	−0.7435	0.6680

TABLE VIII. Initial populations in the i,J levels of $(2p)^5(3d)^9$ due to L_1 and L_2 Coster-Kronig decay. The population produced by L_1 decay was calculated with the ion potential. The first (second) L_2 entry was calculated with the ion (neutral-atom) potential.

Term	Initial populations		
	From L_2 ion	From L_2 neutral	From L_1 ion
$4a$	1.9×10^{-5}	6.8×10^{-6}	3.77
$3a$			2.85
$3b$	0.49	6.87	2.57
$3c$	0.72	12.63	1.55
$2a$			0.44
$2b$			1.59
$2c$	8.24	12.00	0.38
$2d$	4.82	1.50	0.44
$1a$			0.30
$1b$	0.25	0.3	0.43
$1c$	1.07	1.5	0.30
$0a$	0.81	0.29	0.15

TABLE IX. Transition rates from i,J terms of $(2p)^5(3d)^9$ to P_3Q_3 terms of $(2p)^6(3d)^7$.

i,J \ P_3Q_3	^4F −2.94	^4P −0.60	^2H 0.17	^2G −0.61	^2F 2.52	$^2D_1$ 4.48	$^2D_2$ 1.58	^2P 0.17	Total rate (10^{-4}/atu)	Γ (eV)
4*a* −7.87	12.3	0.64	15.5	7.10	4.30	3.89	3.09	2.64	200	0.54
3*a* 21.77	5.43	1.98	49.0	12.5	9.94	3.86	3.00	4.16	249	0.68
3*b* −5.14	3.42	2.25	59.2	13.7	11.8	3.84	2.93	4.67	264	0.72
3*c* −7.23	7.90	4.96	38.3	21.7	5.74	4.70	4.58	2.76	250	0.68
2*a* 21.28	12.3	3.35	20.6	17.2	26.2	8.20	12.6	1.68	262	0.71
2*b* 19.99	9.81	0.83	14.8	15.0	6.44	4.13	6.76	2.49	212	0.58
2*c* −6.52	11.1	4.80	30.3	19.6	21.9	7.65	10.3	1.95	270	0.73
2*d* −7.96	3.86	0.98	11.2	33.9	11.4	4.66	15.8	2.16	240	0.65
1*a* 22.31	5.25	3.89	25.2	25.4	17.5	17.4	6.90	2.10	257	0.70
1*b* −4.76	5.23	1.88	12.1	22.2	21.7	22.9	7.20	1.82	250	0.68
1*c* −6.19	14.3	3.52	20.6	12.7	29.9	9.43	12.0	10.5	273	0.74
0*a* −5.91	20.2	0.77	1.08	0.44	43.4	11.1	15.6	0.80	251	0.68

and experiment in locating peak E. Thus my location of the L_3-$M_{4,5}M_{4,5}$ satellite spectrum relative to the principal spectrum is consistent with the location of the L_2-$M_{4,5}M_{4,5}$ satellite spectrum.

Finally, in Fig. 3 I show the results using the populations in Table VIII obtained with the neutral-atom potential for the L_3-$L_3M_{4,5}$ transition, but with all other matrix elements obtained with the ion potential. The synthesized spectrum in Fig. 3 is in excellent agreement with the measurements of Antonides *et al.*[6] near peak C. The calculation slightly underestimates peak B, but this could be due to the neglect of configuration interaction between $(3p)^6(3d)^8\,{}^1S_0$ and $(3p)^4(3d)^{10}\,{}^1S_0$. At worst, there is quantitative agreement in shape between the calculated and measured Cu L_3-$M_{4,5}M_{4,5}$ satellite spectra in Fig. 3, and semiquantitative agreement in intensity. However the Cu L_2-$L_3M_{4,5}$ rate that leads to agreement between calculated and measured satellite spectra also leads to an L_2 linewidth significantly larger than the measured value.[7]

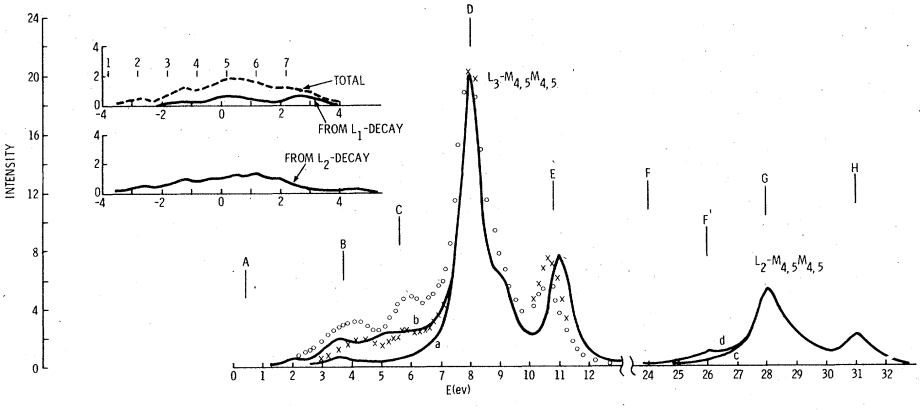

FIG. 2. Synthesized $L_3-M_{4,5}M_{4,5}$ spectra using the ion potential throughout. The inserts on the left show the satellite spectra. The positions A–H locate significant structure as measured in Ref. 4. The curves labeled a and c are the calculated principal spectra, while b and d include the satellite spectra. The circles and crosses are the measurements of Ref. 6, for Cu and Zn, respectively.

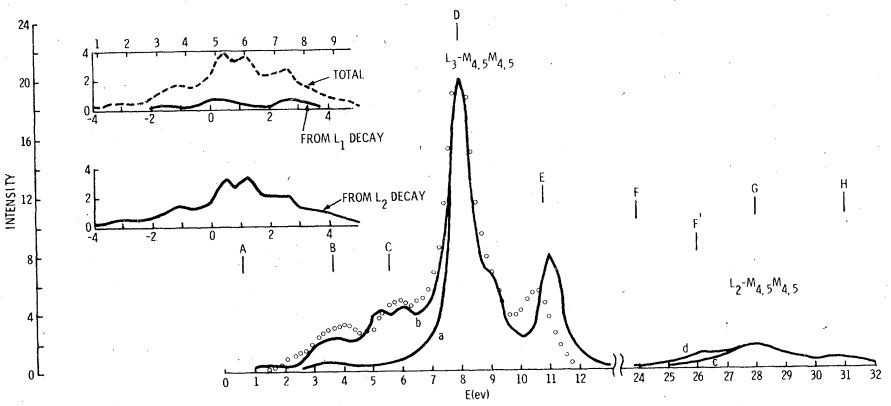

FIG. 3. Synthesized $L_3-M_{4,5}M_{4,5}$ spectra, with $L_3M_{4,5}$ populations from L_2 Coster-Kronig decay calculated with the neutral-atom potential, and ion-potential results used otherwise. The labeling is identical to that in Fig. 2.

IV. CONCLUSIONS

From this attempt to synthesize the CuL_{23}-$M_{4,5}M_{4,5}$ Auger spectra with an atomic description several conclusions emerge. First, the quantitative agreement in the shape of the satellite spectra in both Cu and Zn supports the atomic description in solid Cu of not only the $(2p)^6(3d)^8$ configuration, with two valence holes, but also of both the $(2p)^5(3d)^9$ and $(2p)^6(3d)^7$ configurations; that is, the satellite shape depends on the term structure in both initial and final states, with one and three valence holes, respectively. Second, in treating L_2-L_3X transitions one cannot neglect the electrostatic interaction in the L_3X terms, particularly at low Z and possibly at large Z. When the L_2-$L_3M_{4,5}$ transition rate is calculated in j-j coupling the large matrix element $D(0,2)$ does not affect the calculated rate. In intermediate coupling $D(0,2)$ siginficantly modifies the calculated L_2-$L_3M_{4,5}$ rate. Third, the calculated CuL_3-$M_{4,5}M_{4,5}$ satellite spectra is in good agreement with the measurements only when matrix elements obtained with a neutral-atom potential are used. Matrix elements calculated with a ion potential and incorporated into an intermediate coupling treatment underestimate the CuL_3-$M_{4,5}M_{4,5}$ satellite spectrum. On the other hand, matrix elements calculated with the ion potential do reproduce the observed Zn L_3-$M_{4,5}M_{4,5}$ satellite spectrum. Fourth, the CuL_2-$L_3M_{4,5}$ Coster-Kronig transition rate calculated with the ion potential is consistent with measurements on the widths of CuL_2 and L_3 photoelectron lines. The Coster-Kronig rate calculated with the neutral-atom potential leads to a calculated L_2 linewidth far larger than the measured value. Fifth, one cannot do quantitative analysis on the L_2-$L_3M_{4,5}$ Coster-Kronig transition rate via the L_3-$M_{4,5}M_{4,5}$ satellite spectra without correcting for effects due to L_1 vacancy decay. The sequence $L_1 \rightarrow L_{2,3}M_{4,5} \rightarrow (M_{4,5})^3$ has been included in the synthesis, but sequences of the form $L_1 \rightarrow L_{23}M_i(i \neq 4,5) \rightarrow M_i(M_{4,5})^2$ have not been included and can lead to additional staellite structure.

ACKNOWLEDGMENT

I wish to thank H. Madden for his encouragement and interest in these calculations, P. Weightman for providing unpublished data, and E. Antonides for an invaluable preprint. This work was supported by the U. S. Energy Research and Development Administration.

APPENDIX

To obtain Eq. (6) one evaluates Eq. (17) of Ref. 14 in the limit $L_RS_R = P_1Q_1 = {}^1S$, i.e., the $2p$ shell is filled in the final state and the passive electron structure can be neglected. The result is

$$\frac{W_{if}}{2\pi}(17) = \frac{(2P_3+1)(2Q_3+1)(2J+1)(2J_{12}+1)(2j_2+1)}{(2L_3+1)(2S_3+1)} \prod_{i=1}^{4}(2l_i+1)\sum_{C_2}(2C_2+1)$$

$$\times \left| \tfrac{1}{2}[(n+1)(n+2)]^{1/2} \sum_{P_3'Q_3'} (-1)^{2J_{12}-2S_3}[(2P_3'+1)(2Q_3'+1)]^{1/2}(l_3^{n+2}P_3Q_3\{\,|\,l_3^{n+1}P_3'Q_3')(l_3^{n+1}P_3'Q_3'\{\,|\,l_3^nL_3S_3)\right.$$

$$\times \sum_{fgdd_1b} (-1)^{2d+2d_1-f}(2f+1)(2g+1)(2d+1)(2d_1+1)(2b+1) \begin{Bmatrix} J & J_{12} & C_2 \\ j_1 & b & j_2 \end{Bmatrix} \begin{Bmatrix} \frac{1}{2} & \frac{1}{2} & f \\ S_3 & Q_3 & d_1 \end{Bmatrix} \begin{Bmatrix} l_2 & l_1 & g \\ L_3 & P_3 & d \end{Bmatrix}$$
$$\times \begin{Bmatrix} P_3 & P_3' & l_3 \\ l_3 & g & L_3 \end{Bmatrix} \begin{Bmatrix} Q_3 & Q_3' & \frac{1}{2} \\ \frac{1}{2} & f & S_3 \end{Bmatrix} \begin{Bmatrix} l_2 & \frac{1}{2} & j_2 \\ P_3 & Q_3 & J \\ d & d_1 & b \end{Bmatrix} \begin{Bmatrix} l_1 & d & L_3 \\ \frac{1}{2} & d_1 & S_3 \\ j_1 & b & C_2 \end{Bmatrix} I(KK'fg) \Bigg|^2 . \quad \text{(A1)}$$

Next, sum over the irrelevant quantum number J_{12} (obtained by coupling j_1 to the irrelevant continuum electron quantum number j_2) to bring the sum on b outside the absolute value signs. Then, sum the resulting expression over j_2 and J [J can be summed over as spin-orbit splitting of the $(l_3)^{n+2}P_3Q_3$ terms is neglected]. This leads to

$$\sum_{J_{12},j_2,J} \frac{W_{if}(17)}{2\pi} = \frac{(2P_3+1)(2Q_3+1)}{(2L_3+1)(2S_3+1)} \prod_{i=1}^{4}(2l_i+1) \sum_{C_2}(2C_2+1) \sum_{b,d,d_1}(2b+1)(2d+1)(2d_1+1)$$
$$\times \Bigg| \tfrac{1}{2}[(n+1)(n+2)]^{1/2} \sum_{P_3'Q_3'} (-1)^{-2S_3}[(2P_3'+1)(2Q_3'+1)]^{1/2}(l_3^{n+2}P_3Q_3\{\,|\,l_3^{n+1}P_3'Q_3')(l_3^{n+1}P_3'Q_3'\{\,|\,l_3^n L_3S_3)$$
$$\times \sum_{fg}(-1)^{2d+2d_1-f}(2f+1)(2g+1) \begin{Bmatrix} \frac{1}{2} & \frac{1}{2} & f \\ S_3 & Q_3 & d_1 \end{Bmatrix} \begin{Bmatrix} l_2 & l_1 & g \\ L_3 & P_3 & d \end{Bmatrix} \begin{Bmatrix} P_3 & P_3' & l_3 \\ l_3 & g & L_3 \end{Bmatrix}$$
$$\times \begin{Bmatrix} Q_3 & Q_3' & \frac{1}{2} \\ \frac{1}{2} & f & S_3 \end{Bmatrix} \begin{Bmatrix} l_1 & d & L_3 \\ \frac{1}{2} & d_1 & S_3 \\ j_1 & b & C_2 \end{Bmatrix} I(KK'fg) \Bigg|^2 . \quad \text{(A2)}$$

This is the transition rate for a state with initial statistical weight $(2j_1+1)(2L_3+1)(2S_3+1)$. When we substitute $d \to L, d_1 \to S, C_2 \to J_3, b \to J$, we have the transition rate for the initial coupling in terms of a sum over the transition rates in a scheme where we couple l_1 and L_3 to form L, $\frac{1}{2}$ and S_3 to form S, and L and S to form J. Then, if we want the transition rate in the LSJ scheme we drop the sums over $LSJJ_3$ and multiply by $(2L_3+1)(2S_3+1)(2j_1+1)/(2J+1)$ to determine the new transition rate. In j-j coupling the result we seek is obtained by summing over L and S, but not j_1 and J_3.

$$\frac{W_{if}(j_1,J_3,J,P_3Q_3)}{2\pi} = (2P_3+1)(2Q_3+1)(2j_1+1)(2J_3+1) \sum_{L,S}(2L+1)(2S+1) \prod_{i=1}^{4}(2l_i+1)$$
$$\times \Bigg| \tfrac{1}{2}[(n+1)(n+2)]^{1/2} \sum_{P_3'Q_3'} [(2P_3'+1)(2Q_3'+1)]^{1/2}(l_3^{n+2}P_3Q_3\{\,|\,l_3^{n+1}P_3'Q_3')(l_3^{n+1}P_3'Q_3'\{\,|\,l_3^n L_3S_3)$$
$$\times \sum_{f,g}(-1)^{2L+2S-f}(2f+1)(2g+1) \begin{Bmatrix} \frac{1}{2} & \frac{1}{2} & f \\ S_3 & Q_3 & S \end{Bmatrix} \begin{Bmatrix} l_2 & l_1 & g \\ L_3 & P_3 & L \end{Bmatrix}$$
$$\times \begin{Bmatrix} P_3 & P_3' & l_3 \\ l_3 & g & L_3 \end{Bmatrix} \begin{Bmatrix} Q_3 & Q_3' & \frac{1}{2} \\ \frac{1}{2} & f & S_3 \end{Bmatrix} \begin{Bmatrix} l_1 & L & L_3 \\ \frac{1}{2} & S & S_3 \\ j_1 & J & J_3 \end{Bmatrix} I(KK'fg) \Bigg|^2 . \quad \text{(A3)}$$

But in Ref. 17 we define

$$\frac{W_{if}(LS,PQ)}{2\pi} = \tfrac{1}{4}(n+1)(n+2) \prod_{i=1}^{4}(2l_i+1)(2P+1)(2Q+1)$$
$$\times \Bigg| \sum_{f,g}(-1)^g(2f+1)(2g+1)I(KK'fg) \begin{Bmatrix} \frac{1}{2} & \frac{1}{2} & f \\ S_3 & Q & S \end{Bmatrix} \begin{Bmatrix} l_2 & l_1 & g \\ L_3 & P & L \end{Bmatrix}$$

$$\times \sum_{P'Q'} \sqrt{(2P'+1)(2Q'+1)} \begin{Bmatrix} P & P' & l_3 \\ l_3 & g & L_3 \end{Bmatrix} \begin{Bmatrix} Q & Q' & \frac{1}{2} \\ \frac{1}{2} & f & S_3 \end{Bmatrix}$$

$$\times (l_3^{n+2} PQ\{|l_3^{n+1} P'Q')(l_3^{n+1} P'Q'\{|l_3^n L_3 S_3)\Big| . \quad \text{(A4)}$$

Since $f+g$ is even for the equivalent electron case we have

$$\frac{W_{if}(j_1 J_3, P_3 Q_3)}{2\pi} = \sum_{L,S} (2L+1)(2S+1) \frac{W_{if}(LS, P_3 Q_3)}{2\pi} \left| [(2j_1+1)(2J_3+1)]^{1/2} \begin{Bmatrix} l_1 & L & L_3 \\ \frac{1}{2} & S & S_3 \\ j_1 & J & J_3 \end{Bmatrix} \right|^2 . \quad \text{(A5)}$$

Finally, in intermediate coupling one has $\sum_{j_1 J_3} C_i(j_1 J_3 J)$ inside the absolute value signs so that

$$\frac{W_{if}(iJ, P_3 Q_3)}{2\pi} = \sum_{LS} (2L+1)(2S+1) \frac{W_{if}(LS, P_3 Q_3)}{2\pi} \left| \sum_{j_1', J_3} C_i(j_1' J_3 J)[(2j_1'+1)(2J_3+1)]^{1/2} \begin{Bmatrix} l_1 & L & L_3 \\ \frac{1}{2} & S & S_3 \\ j_1' & J & J_3 \end{Bmatrix} \right|^2 . \quad \text{(A6)}$$

[1] L. I. Yin, T. Tsang, I. Adler, and E. Yellin, J. Appl. Phys. 43, 3464 (1972).
[2] G. Schön, J. Electron. Spectrosc. 1, 377 (1972).
[3] S. P. Kowalczyk, R. A. Pollak, F. R. McFeely, L. Ley, and D. A. Shirley, Phys. Rev. B 8, 2387 (1973).
[4] E. D. Roberts, P. Weightman, and C. E. Johnson, J. Phys. C 8, L301 (1975).
[5] E. Antonides, E. C. Janse, and G. A. Sawatzky, Phys. Rev. B 15, 1669 (1977).
[6] E. Antonides, E. C. Janse, and G. A. Sawatzky, Phys. Rev. B 15, 4596 (1977).
[7] L. I. Yin, I. Adler, M. H. Chen, and B. Crasemann, Phys. Rev. A 7, 897 (1973).
[8] L. I. Yin, I. Adler, T. Tsang, M. H. Chen, D. A. Ringers, and B. Crasemann, Phys. Rev. A 9, 1070 (1974).
[9] P. A. Feibelman and E. J. McGuire, Phys. Rev. B 15, 3575 (1977).
[10] P. A. Feibelman, Bull. Am. Phys. Soc. 22, 432 (1977).
[11] P. Weightman, J. F. McGilp, and C. E. Johnson, J. Phys. C 9, L585 (1976).
[12] D. W. Nix and R. W. Fink, Z. Physik, 273, 305 (1975).
[13] W. N. Asaad, Nucl. Phys. 44, 415 (1963).
[14] E. J. McGuire, in *Atomic Inner Shell Processes*, edited by B. Crasemann (Academic, New York, 1975).
[15] J. C. Slater, *Quantum Theory of Atomic Structure* (McGraw-Hill, New York, 1960).
[16] J. B. Mann, Los Alamos Scientific Laboratory Report No. LASL-3690 (1967) (unpublished).
[17] E. J. McGuire, Phys. Rev. A 10, 32 (1974).
[18] E. J. McGuire, Sandia Research Report No. SC-RR-70-721 (unpublished).
[19] E. J. McGuire, Sandia Research Report No. SC-RR-71-0075 (unpublished).
[20] The quantity $-rV/r$ calculated in Ref. 21 is approximated by a series of N piecewise-continuous straight lines. Both discrete and continuum orbitals for the Schrödinger equation are obtained in terms of Whittaker functions. The procedure is discussed in E. J. McGuire, Phys. Rev. 175, 20 (1968).
[21] F. Herman and S. Skillman, *Atomic Structure Calculations* (Prentice-Hall, Englewood Cliffs, N. J., 1963).
[22] D. L. Walters and C. P. Bhalla, Phys. Rev. A 4, 2164 (1971).
[23] S. Aksela and H. Aksela, Phys. Lett. 48A, 19 (1974).
[24] The matrix elements are in units of 0.01 inverse Bohr radii. The continuum orbitals used were normalized per Rydberg rather than per Hartree, so either all the matrix elements should be multiplied by $\sqrt{2}$, or equivalently the factor 2π in the transition-rate expression should be replaced by 4π.